JAAS

PAPER

View Article Online
View Journal | View Issue

Cite this: J. Anal. At. Spectrom., 2021, 36, 999

^{238}U–^{206}Pb dating of U-series disequilibrium zircons by secondary ion mass spectrometry†

Yong-Shu Huang,[abc] Qiu-Li Li, *[abc] Yu Liu, [ac] Ping-Ping Liu,[d] Sun-Lin Chung[e] and Xian-Hua Li [abc]

Determining the timescales of magma accumulation and storage prior to large eruptions is fundamental to understand the pre-eruptive history of magma reservoirs. Zircon ^{238}U–^{230}Th dating has been widely used to recover the timescales of magma reservoirs younger than 400 ka. However, theoretically and practically, the uncertainties for zircons older than *ca.* 150 ka, *i.e.*, two half-lives of ^{230}Th, are large because (^{238}U)/(^{230}Th) activities start to stabilize. On the other hand, the accumulation of radiogenic ^{206}Pb begins to increase significantly after two half-lives of ^{230}Th. Herein we theoretically demonstrate a calibration method for SIMS (Secondary Ion Mass Spectrometry) ^{238}U–^{206}Pb dating within the timescales of U-series disequilibrium and apply it to zircons of the 75 ka Youngest Toba Tuff (YTT) in northern Sumatra, Indonesia. The ^{238}U–^{206}Pb dates vary from *ca.* 665 to 75 ka after common Pb and initial ^{230}Th disequilibrium corrections. This age range agrees with that obtained by previous studies using the ^{238}U–^{230}Th method, but the precision of each age is improved by a factor of three or more. ^{238}U–^{206}Pb and ^{238}U–^{230}Th dating methods have advantages and disadvantages for zircons in U-series disequilibrium. The ^{238}U–^{230}Th method is more suited to samples younger than 150 ka, but requires a large Th/U fractionation between the zircon and magma, and a high U content. The ^{238}U–^{206}Pb method is more appropriate for samples older than 150 ka, but requires high U and low common Pb contents. Our approach improves the precision of *in situ* dating of zircon in U-series disequilibrium, which will contribute to investigations of the magmatic evolution beneath young volcanoes.

Received 15th December 2020
Accepted 17th March 2021

DOI: 10.1039/d0ja00510j

rsc.li/jaas

1. Introduction

Zircon is the most widely used U–Pb geochronometer because: (1) it contains abundant U and Th and does not incorporate Pb during crystallization; (2) it is very stable and resistant to disturbance by later hydrothermal activity and weathering; (3) it is widely distributed in most crustal rocks; (4) it can be used to investigate the history of the lithosphere together with a range of geochemical proxies. Given these properties, the U–Pb dating of zircon in young volcanic rocks can be used to investigate magmatic evolution in crustal magma chambers.[1–4]

For young samples within the time-scale of U-series disequilibrium, radiogenic lead is only a part of radiogenic daughters decayed from uranium because of a number of intermediate nuclides with varying half-lives. In a U-bearing magmatic system that has remained undisturbed for ~0.5 Ma, a state of secular equilibrium becomes established between the abundance of parent and daughter nuclides in the U-series decay chain, such that the decay rate (or "activity") of each intermediate daughter nuclide in the chain is equal to that of the parent.[5] During the crystallization of zircon in magma, nuclides in the U-series decay chain can become fractionated relative to one another, due to their different chemical properties or the lattice sites they occupy. This results in U-series disequilibrium, which can be utilized as dating tools. The ^{238}U–^{230}Th system is most widely used for the study of igneous systems that are in U-series disequilibrium.[1,6,7] The applicable age range of ^{238}U–^{230}Th dating is *ca.* 400 ka, based on the assumption that its activity will be within the error of secular equilibrium after five half-lives of ^{230}Th. However, the dating uncertainty will increase gradually as the (^{238}U)/(^{230}Th) activities begin to change less after two half-lives of ^{230}Th (*ca.* 150 ka). Interestingly, the abundance of radiogenic ^{206}Pb in zircon begins to surpass that of ^{230}Th at that time. Though ^{238}U–^{206}Pb dating was never confidentially applied to date zircons within the time scale of U-series disequilibrium, it has potential to improve

[a]State Key Laboratory of Lithospheric Evolution, Institute of Geology and Geophysics, Chinese Academy of Sciences, Beijing 100029, China. E-mail: liqiuli@mail.iggcas.ac.cn
[b]College of Earth and Planetary Sciences, University of Chinese Academy of Sciences, Beijing 100049, China
[c]Innovation Academy for Earth Science, Chinese Academy of Sciences, Beijing 100029, China
[d]Key Laboratory of Orogenic Belts and Crustal Evolution, School of Earth and Space Sciences, Peking University, Beijing 100871, China
[e]Institute of Earth Sciences, Academia Sinica, Taipei

† Electronic supplementary information (ESI) available. See DOI: 10.1039/d0ja00510j

the precision of zircon ages older than 150 ka. However, there are many challenges involved in U–Pb dating such young zircons. The limited radiogenic Pb that has been accumulated may result in a poor precision of the isotopic measurements.[8] In addition, robust correction for common Pb and initial ^{230}Th disequilibrium in young samples under U-series disequilibrium is not straightforward. Therefore, it is necessary to establish a set of calibration and testing methods for ^{238}U–^{206}Pb dating on zircon within the time scale of U-series disequilibrium.

In this paper, we first theoretically derive the formulae that include the common Pb and initial ^{230}Th disequilibrium corrections for U-series disequilibrium and develop an analytical protocol for ion microprobe U–Pb dating of young zircon. We then present ^{238}U–^{206}Pb dating results for zircons extracted from the 75 ka YTT collected from around the Toba Caldera in northern Sumatra, Indonesia. Our corrected results are consistent with the age range obtained by previous ^{238}U–^{230}Th studies,[4] but have significantly improved precision, which verifies our correction protocols. In addition, we evaluate the applicability and the advantages and disadvantages of zircon ^{238}U–^{206}Pb and ^{238}U–^{230}Th dating.

2. Calibration protocols

An excess or deficit of intermediate nuclides incorporated during zircon crystallization from young magma would result in an erroneous U–Pb date, and thus a correction for the presence of initial intermediate nuclides is essential. Given that the abundance of a nuclide is directly proportional to its half-life (*i.e.*, inversely proportional to its decay constant), intermediate nuclides with short half-lives have little effect on dating. The negligible fractionation between ^{238}U and ^{234}U in the magmatic system can also be ignored. In the U-series decay chain, ^{230}Th has a relatively long half-life and its initial disequilibrium can significantly affect the final U–Pb dating result. Owing to Th–U fractionation during zircon crystallization, zircon usually has a lower Th/U ratio than the magma. The deficit of ^{230}Th in zircon slows down the growth of radiogenic ^{206}Pb*, which results in younger U–Pb ages.[9] Therefore, an initial ^{230}Th disequilibrium correction is essential for obtaining reliable ^{238}U–^{206}Pb ages. The common Pb correction is another important issue because of the limited amount of radiogenic Pb* in young zircons.

2.1 ^{230}Th disequilibrium correction

A simplified schematic diagram of the U-series decay chain is shown in Fig. 1a. The radiogenic daughter (D*) of ^{238}U contains three components: the radiogenic daughter $^{206}Pb_U$, the intermediate nuclide $^{230}Th_U$ from the decay of ^{238}U, and negligible amounts of short half-life daughters (Fig. 1b). In addition, the initial $^{230}Th_0$ incorporated during the crystallization of zircons decays to $^{206}Pb_{Th}$ afterwards. Together with $^{206}Pb_U$, they constitute the radiogenic ^{206}Pb* (Fig. 1a). Therefore, the measured $^{206}Pb_m$ contains three components: the $^{206}Pb_U$ derived from the decay of ^{238}U, the $^{206}Pb_{Th}$ derived from the decay of initial $^{230}Th_0$ and the common ^{206}Pb (*i.e.*, $^{206}Pb_c$) (Fig. 1c). Therefore, the radiogenic daughter (D*) of ^{238}U can be determined from the following equation:

$$D^* = {}^{206}Pb_m - {}^{206}Pb_{Th} + {}^{230}Th_U - {}^{206}Pb_c \quad (1)$$

By assuming that the magma is in secular equilibrium, the initial $^{230}Th_0$ and $(^{230}Th/^{238}U)_0$ of zircon can be calculated from the following equations:

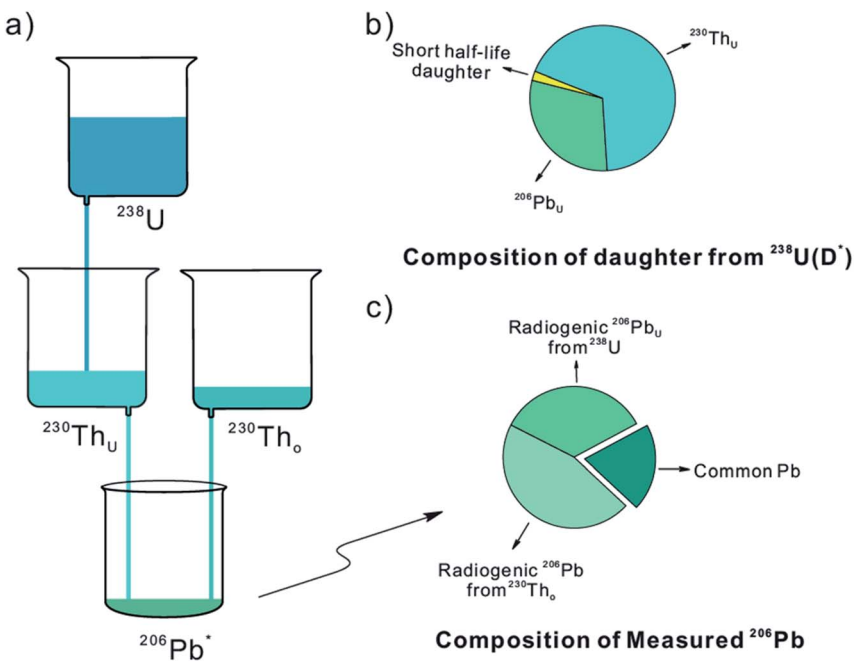

Fig. 1 (a) Simplified diagram of the U-series decay chain; (b) composition of the daughters of ^{238}U; (c) composition of the measured ^{206}Pb.

$$^{230}\mathrm{Th}_0 = \mathrm{Th}_{\mathrm{zir}} \times \frac{^{230}\mathrm{Thmag}}{\mathrm{Th}_{\mathrm{mag}}} = \mathrm{Th}_{\mathrm{zir}} \frac{^{238}\mathrm{Umag}(\lambda_{238}/\lambda_{230})}{\mathrm{Th}_{\mathrm{mag}}} \quad (2)$$

$$\left(\frac{^{230}\mathrm{Th}}{^{238}\mathrm{U}}\right)_0 = \frac{\lambda_{238}}{\lambda_{230}} \times f_{\mathrm{Th/U}} \quad (3)$$

$$f_{\mathrm{Th/U}} = \frac{(\mathrm{Th/U})_{\mathrm{zir}}}{(\mathrm{Th/U})_{\mathrm{mag}}} \quad (4)$$

where $^{230}\mathrm{Th}_{\mathrm{zir}}$ and $^{238}\mathrm{U}_{\mathrm{zir}}$ are the ^{230}Th and ^{238}U contents of zircon, $^{230}\mathrm{Th}_{\mathrm{mag}}$ and $\mathrm{Th}_{\mathrm{mag}}$ are the ^{230}Th and Th contents of magma, and λ_{238} and λ_{230} are the decay constants of ^{238}U and ^{230}Th ($\lambda_{238} = 1.55125 \times 10^{-10}$ per year and $\lambda_{230} = 9.195 \times 10^{-6}$ per year). $f_{\mathrm{Th/U}}$ is the fractionation factor of Th/U between zircon and melt, which can be calculated from the Th/U ratios of zircon and magma. The Th/U ratio of zircon can be measured directly, whereas the Th/U ratio of magma is normally represented by that of the whole rock or volcanic glass. The $^{206}\mathrm{Pb}_{\mathrm{Th}}$ produced from radioactive decay of initial $^{230}\mathrm{Th}_0$ can be expressed as:

$$^{206}\mathrm{Pb}_{\mathrm{Th}} = {}^{230}\mathrm{Th}_0(1 - \mathrm{e}^{-\lambda_{230}t}) \quad (5)$$

By combining eqn (1)–(5), we obtain an expression describing the (D/^{238}U) ratio and age (t):

$$\frac{D}{^{238}\mathrm{U}} = \frac{^{206}\mathrm{Pbc}}{^{238}\mathrm{U}} + (\mathrm{e}^{\lambda_{238}t} - 1) + \frac{\lambda_{238}}{\lambda_{230}}(1 - \mathrm{e}^{-\lambda_{238}t})\left(f_{\mathrm{Th/U}} - 1\right)\mathrm{e}^{\lambda_{238}t} \quad (6)$$

where D represents the total amount of decay daughters of ^{238}U and common lead ($D = D^* + {}^{206}\mathrm{Pb}_c$).

2.2 Common lead correction

The common Pb correction involves calculating the proportion of common Pb relative to total ^{206}Pb, *i.e.*, f_{206}, where total ^{206}Pb is the sum of common and radiogenic Pb. Radiogenic Pb is treated as being solely derived from the decay of ^{238}U (D^*) for samples in secular equilibrium, but not suitable for zircons in U-series disequilibrium. Thus, we use D to represent the total radiogenic daughters of ^{238}U (D^*) plus common Pb:

$$f_{206} = \frac{^{206}\mathrm{Pbc}}{D} \quad (7)$$

Having determined the proportion of common Pb, the ratio between the radiogenic daughter and ^{238}U can be determined as

$$\frac{D^*}{^{238}\mathrm{U}} = \frac{D}{^{238}\mathrm{U}} \cdot (1 - f_{206}) \quad (8)$$

Typically, the proportion of common Pb (f_{206}) can be calculated from the non-radiogenic ^{204}Pb. However, due to the low ^{204}Pb abundance of zircon and potential isobaric interference during measurement, the ^{204}Pb correction can result in large uncertainties. Fortunately, ^{207}Pb/^{206}Pb ratios vary little (0.058–0.046) since the Phanerozoic and the signal intensity of ^{207}Pb is about 15 times higher than that of ^{204}Pb, which significantly improves the analytical precision.[10] Therefore, the ^{207}Pb-based common Pb correction is superior for young zircons and can be expressed as:

$$f_{206} = \frac{\left(\frac{^{207}\mathrm{Pb}}{D}\right)_m - \left(\frac{^{207}\mathrm{Pb}}{^{206}\mathrm{Pb}}\right)^*}{\left(\frac{^{207}\mathrm{Pb}}{^{206}\mathrm{Pb}}\right)_c - \left(\frac{^{207}\mathrm{Pb}}{^{206}\mathrm{Pb}}\right)^*} \quad (9)$$

where the subscript m represents the measured value and the superscript * represents the ratio of radiogenic Pb. Based on a two-stage Pb evolution model of the Earth,[11] the modern terrestrial Pb isotopic composition (0.84 ± 0.05) was used to estimate the composition of common Pb. (^{207}Pb/^{206}Pb)* represents the ratio of total radiogenic daughter of ^{235}U and total radiogenic daughter of ^{238}U, and the present-day value of 0.046 is used in the calculations. In eqn (9), (D/^{207}Pb)$_m$ can be expressed as:

$$\left(\frac{D}{^{207}\mathrm{Pb}}\right)_m = \left(\frac{^{206}\mathrm{Pb}}{^{207}\mathrm{Pb}}\right)_m + \left(\frac{^{206}\mathrm{Pb}}{^{207}\mathrm{Pb}}\right)_m \left(\frac{^{238}\mathrm{U}}{^{206}\mathrm{Pb}_m}\right)\left(\frac{\lambda_{238}}{\lambda_{230}}(1 - \mathrm{e}^{-\lambda_{230}t})\left(1 - f_{\mathrm{Th/U}}\right)\right)\mathrm{e}^{-\lambda_{238}t} \quad (10)$$

After solving eqn (1)–(10) and using the approximation $\lambda_{230} - \lambda_{238} \approx \lambda_{230}$, we obtain an equation describing the relationship between the age (t) and the ratio of D^*/^{238}U:

$$\frac{D^*}{^{238}\mathrm{U}} = \frac{\alpha}{\left(\frac{^{207}\mathrm{Pb}}{^{206}\mathrm{Pb}}\right)_c - \left(\frac{^{207}\mathrm{Pb}}{^{206}\mathrm{Pb}}\right)^*}\left(\left(\frac{^{206}\mathrm{Pb}}{^{238}\mathrm{U}}\right)_m + \frac{\lambda_{238}}{\lambda_{230}}(1 - \mathrm{e}^{-\lambda_{230}t})\left(1 - f_{\mathrm{Th/U}}\right)\right)\mathrm{e}^{\lambda_{238}t} \quad (11)$$

$$\text{where } \alpha = \left(\frac{^{207}\mathrm{Pb}}{^{206}\mathrm{Pb}}\right)_c - \frac{\left(\frac{^{207}\mathrm{Pb}}{^{206}\mathrm{Pb}}\right)_m}{1 + \left(\frac{^{238}\mathrm{U}}{^{206}\mathrm{Pb}_m}\right)\left(\frac{\lambda_{238}}{\lambda_{230}}(1 - \mathrm{e}^{-\lambda_{230}t})\left(1 - f_{\mathrm{Th/U}}\right)\right)\mathrm{e}^{\lambda_{238}t}}$$

3. Sample analysis

3.1 Sample description

Samples were collected from the Toba Caldera, which is located in the Barisan Mountains in northern Sumatra, West Indonesia. Toba is situated on the Sunda Arc and has produced four major eruptions in its history, including the Haranggoal Dacite Tuff (HDT) at 1.2 Ma,[12] the Oldest Toba Tuff (OTT) at 0.84 Ma,[13] the Middle Toba Tuff (MTT) at 0.5 Ma,[14] and the Youngest Toba Tuff (YTT) at 0.074 Ma.[15] We collected rock samples (14SU51 and 14SU03) with a whole-rock Th/U ratio of 3.2 from the most recent YTT eruption. The rhyolitic tuff has variable SiO_2 contents (68–76 wt%) and contains phenocrysts of quartz, plagioclase, K-feldspar, mica, and amphibole. Some plagioclase and amphibole are probably xenocrysts derived from rocks as old as 1.5 Ma.[16]

3.2 Analytical methods

3.2.1 Sample preparation. The zircons were separated by conventional methods and euhedral crystals were handpicked using a binocular microscope. The selected zircons and standards (Plešovice and Qinghu) were placed on double-sided sticky tape and then embedded in a one-inched diameter epoxy resin mount. The mount was polished down to expose the mid-sections of the zircon crystals. Transmitted and reflected light photomicrographs and cathodoluminescence images were obtained to reveal the internal structures of the zircons and guide the site selection. After cleaning with ethanol and deionized water, the mounts were vacuum-coated with ~30 nm of high purity Au to ensure a resistance of <20 Ω across the sample surface.

3.2.2 Instrumental settings. The U–Pb age determination was performed using a CAMECA IMS 1280-HR ion microprobe at the Institute of Geology and Geophysics, Chinese Academy of Sciences, Beijing, China. An O_2^- primary ion beam was accelerated at ~13 kV potential, with an intensity of ~35 nA. The beam spot size is 25 × 35 μm with an elliptical shape. The exit slit is the multi-collector system slit #3, which corresponds to a mass resolution of 8000 (50% peak height). High purity (99.999%) oxygen gas was introduced onto the sample surface (oxygen flooding) to enhance the yield of Pb^+.[17,18] Precisely measuring the Pb isotopic composition of young zircons is challenging because of the low levels of accumulated radioactive Pb. In order to improve the precision of the Pb isotopic measurements, a dynamic multi-collector mode was used with five movable electron multipliers (EMs). Detailed detector configuration and analytical sequences can be referenced to Liu *et al.*[19] Because of the higher yield of UO^+ (twice that of UO_2^+ and six times that of U^+), the intensity of $^{238}UO^+$ exceeds 1×10^6 cps at high primary ion beam intensities. Such high intensities greatly reduce the EM counting precision. Thus, we analyzed $^{235}UO^+$ instead of $^{238}UO^+$. A constant $^{90}Zr_2{}^{16}O^+$ signal was used as the matrix peak to adjust the secondary ion beam energy and mass alignment and calibrate the yields of each EM. The Pb isotope measurements on NIST610 glass were used to check the relative yields of different EMs. Each analysis spot was pre-sputtered over a square area (50 × 50 μm) for 120 s to remove any surface contamination and enhance the yield of secondary ions prior to data acquisition. Each measurement consisted of 10 cycles, with a total analytical time of ~12 min. Every five unknown sample analyses were followed by the analysis of the Plešovice zircon standard. The Qinghu zircon standard was analyzed to monitor the stability of the instrument and the data quality.

3.3 Data processing

The linear relationship between $\ln(^{206}Pb^+/^{238}U^+)$ and $\ln(^{238}U^{16}O_2{}^+/^{238}U^+)$ established by the analyses of the standard zircon Plešovice was used to correct for Pb/U instrumental fractionation. The $^{232}Th/^{238}U$ ratio is calculated from the $^{232}ThO^+/(137.818 \times {}^{235}UO^+)$ ratio[20] in conventional zircon U–Pb analytical procedures. The $f_{Th/U}$ value was calculated based on the Th/U ratios of the whole-rock and zircons. This and the measured $(^{206}Pb/^{238}U)_m$ and $(^{207}Pb/^{206}Pb)_m$ substituted into eqn (11) allow the age of the sample (t) to be determined. However, eqn (11) is a transcendental equation, and was thus solved iteratively. The uncertainties from four factors were propagated into the final age uncertainties: the uncertainties of the measured $^{206}Pb/^{238}U$, measured $^{207}Pb/^{206}Pb$, common Pb ratio (0.84 ± 0.05), and fractionation factor ($f_{Th/U}$). The uncertainty of $f_{Th/U}$ is mainly due to the fact that the magma composition surrounding each zircon grain may not be completely homogeneous and that one volcanic glass or whole-rock Th/U measurement may not represent the actual Th/U ratio of the magma. Therefore, an uncertainty of 50% was assigned to the Th/U ratio of the magma (3.2 ± 1.6).

3.4 Results

During the analyses, even if we used a high primary beam intensity of ~35 nA, ^{207}Pb generated very low signal intensity of 1 cps (average at 4 cps), indicating a very low common Pb content. However, this intensity is far above the noise level of the collector (~0.02 cps), which highlights the reliability of measuring ^{207}Pb in young zircons. The age obtained for the Qinghu standard (160.0 ± 1.3 Ma) is consistent with its recommended value (159.5 ± 0.2 Ma).[21] We obtained 41 magmatic zircon ages from the YTT samples (ESI Table 1† and Fig. 2). The zircon U contents vary from 95 to 1630 ppm, with Th/U ~0.5–1.56 (most are <1). The zircon ^{238}U–^{206}Pb ages range from 665 to 75 ka (Fig. 2).

4. Discussion

4.1 Duration of YTT magma

The 74 ka YTT is the product of a caldera-forming "super-eruption" in northern Sumatra. It records the largest volcanic eruption experienced by the modern human race.[3,4] It has been recognized that there is a broad correlation between the volume of erupted magma and the repose time. Thus, the YTT super-volcano systems were continuously fed by magma, and the magma reservoir grew quiescently until something triggered the eruption. The frequent occurrence of zircon as inclusions in

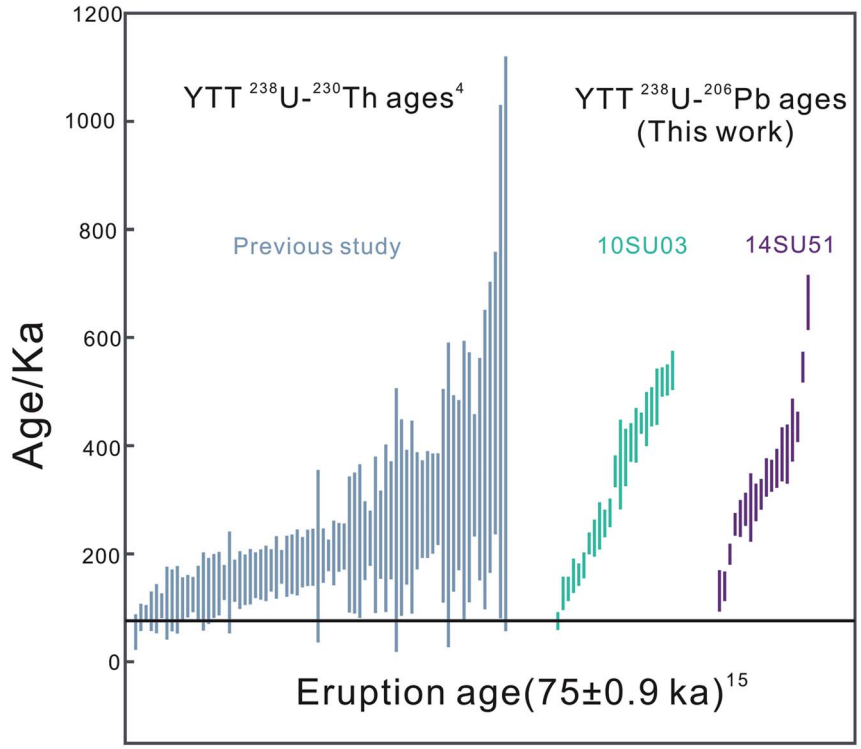

Fig. 2 ^{238}U–^{206}Pb dating results for magmatic zircon from YTT samples obtained in this study compared with ^{238}U–^{230}Th age data[4] (error bars are 2σ).

major phenocryst phases in rhyolites shows that zircon grows prior to eruption. Several features of zircon make it amenable to dating for the magma accumulation history.

Reid and Vazquez[4] investigated the chronological record of zircon crystallization across the entire compositional spectra of the YTT magma reservoir by using ion microprobe U–Th and U–Pb dates. Depth profile analyses revealed that a single zircon crystal could have grown over several hundred ka. Spot analyses provided a better assessment of the overall distributions of crystallization ages for cores and interiors. Based on the crystallization ages recorded by crystal cores, zircons nucleated at various times before but mostly after the MTT eruption (at 501 ka). As for our results, except two zircon grains with slightly older ages than the MTT eruption time, *i.e.*, 545 ± 28 ka and 665 ± 51 ka, other 39 grains show a continuous distribution between 501 and 75 ka. Though both observations look identical, it is important to consider that the resolution of U–Th dates can be poor when U–Th approaches secular equilibrium. Our U–Pb dates improve age precision 3 times better than U–Th dating for zircon >150 ka.

4.2 Effect of the common Pb correction

In the study of Guillong *et al.*,[8] the interference of ^{204}Hg made the ^{204}Pb-based common Pb correction impossible as analyzed by LA-ICP-MS. Even the ^{207}Pb signal was too low to be measured precisely; therefore the common Pb correction was not conducted. However, the proportion of common Pb in most zircons from the YTT analyzed by Reid and Vazquez[4] was >50%. In this study, the analyzed zircons have very low common Pb contents but still high common Pb proportions (average ~15%). Hence, the common Pb correction would significantly affect the accuracy of the dating results. The main difficulty with the ^{204}Pb-based common Pb correction for young zircons is the high f_{206} with large uncertainties due to the low common Pb content. Instead, ^{207}Pb-based common Pb correction is applied to young zircons.

Apart from analytical challenges, to the best of our knowledge, the initial ^{230}Th disequilibrium correction on ^{207}Pb/^{206}Pb$_m$ during the common Pb correction has not been discussed. We compared the differences in ages with and without the initial ^{230}Th disequilibrium correction on ^{207}Pb/^{206}Pb$_m$ (ESI Table 1†). The results show that no initial ^{230}Th disequilibrium correction on ^{207}Pb/^{206}Pb$_m$ generates younger ages. Moreover, the degree of the age difference is related to the zircon age (*i.e.*, younger zircons have a larger age difference [Δt]; Fig. 3). In addition, we also obtained the theoretical age difference (Δt) by fixing the fractionation factor ($f_{Th/U}$) between zircon and melt and the proportion of common Pb (f_{206}; Fig. 3). Notably, the age difference is related not only to the actual zircon age, but also to the $f_{Th/U}$ and f_{206} values. A higher f_{206} or smaller $f_{Th/U}$ results in a greater effect on the age bias. We obtained one zircon age (75.4 ± 16.6 ka; ±2σ) that is consistent with the YTT eruption time.[15] If the initial ^{230}Th disequilibrium correction on ^{207}Pb/^{206}Pb was neglected, a much younger age of 55.8 ± 12.3 ka (±2σ) would be obtained, which is obviously wrong.

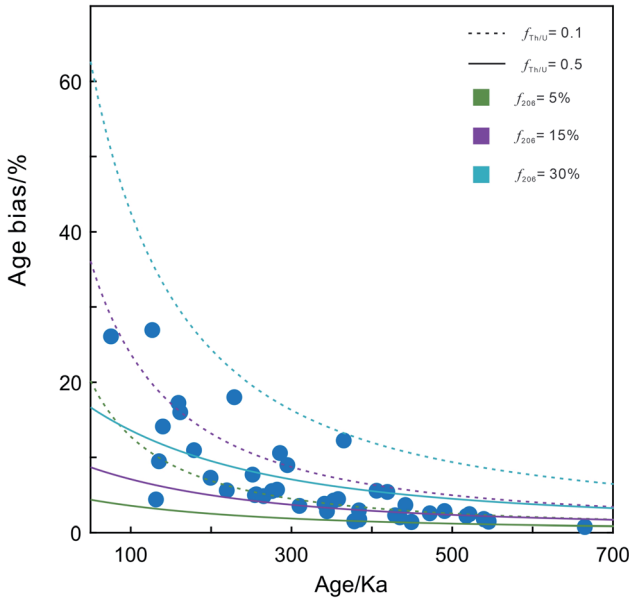

Fig. 3 Relationship between the age differences with and without the initial ^{230}Th disequilibrium correction on ^{207}Pb/^{206}Pb$_{measure}$ and the actual age. The theoretical curves were obtained by fixing the fractionation factor ($f_{Th/U}$) between zircon and melt and the proportion of common Pb (f_{206}). The scattered data points represent the distribution of the measured values.

In the ^{235}U–^{207}Pb decay chain, ^{231}Pa also has a long half-life (32 400 year). Its deficit or excess can also affect the common Pb correction. However, our understanding of the geochemical behavior of ^{231}Pa is limited. Heaman and LeCheminant[22] suggested that the ionic radius of ^{231}Pa is intermediate between those of Th and U; thus its partition coefficient between melt and minerals should also be intermediate between those of Th and U. This implies that initial ^{231}Pa disequilibrium will lead to a deficit of ^{207}Pb. However, Blundy *et al.*[23] showed that ^{231}Pa is very compatible in zircons, based on lattice strain partitioning models. Schmitt[24] found that ^{231}Pa is more compatible than U in zircon, based on the analysis of zircons from the Holocene Salton Buttes rhyolite, but that the initial ^{231}Pa disequilibrium leads to only a slight excess of ^{207}Pb. The low ^{231}Pa content in zircon, which is theoretically ~70 times less than ^{230}Th,[24] is difficult to measure precisely. Therefore, the effect of initial ^{231}Pa disequilibrium was not considered in this study. Based on the consistency of the measured results, it is reasonable to infer that the extent of this effect is negligible at current analytical uncertainties.

4.3 ^{238}U–^{206}Pb *versus* ^{238}U–^{230}Th dating

The U–Pb dating results obtained for the YTT zircons in this study validate that the ^{238}U–^{206}Pb system is applicable to zircon crystallized within the age range of U-series disequilibrium, but the applicable age range needs to be further clarified. Fig. 4a shows the relationship between the ^{230}Th/^{238}U and ^{206}Pb/^{238}U ratios as a function of age. Initially, the zircon ^{206}Pb/^{238}U ratio is much lower than the ^{230}Th/^{238}U ratio. However, the ^{206}Pb/^{238}U ratio will exceed the ^{230}Th/^{238}U ratio after *ca.* 150 ka (about two

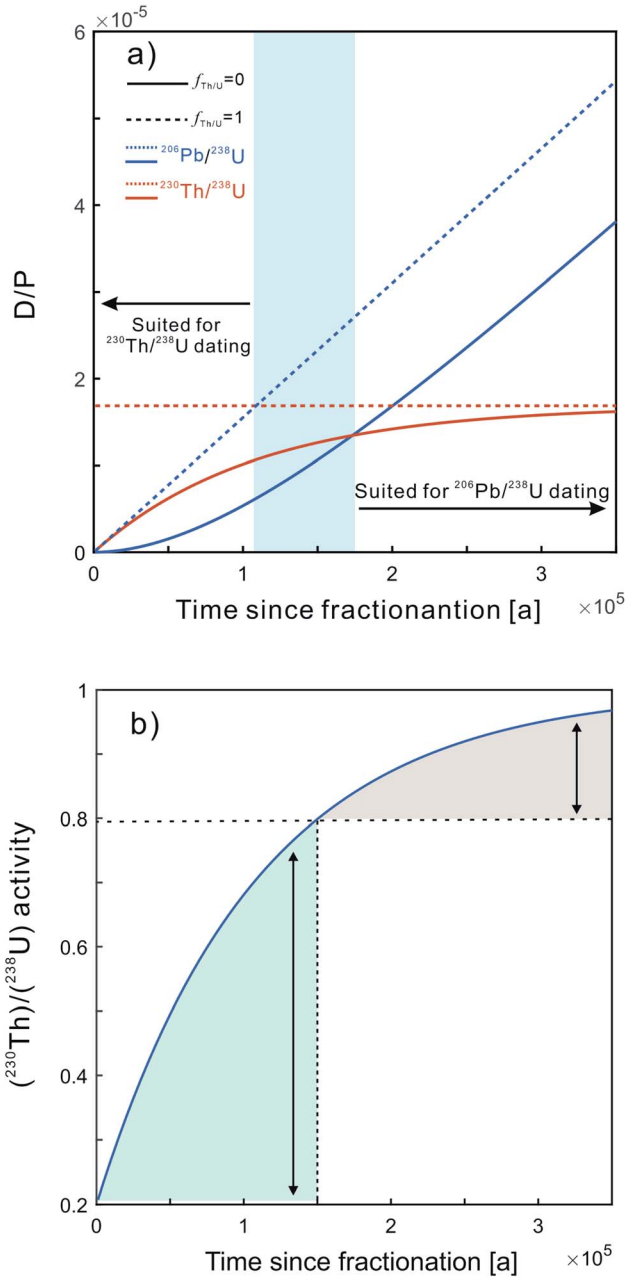

Fig. 4 (a) Growth curves of the ^{230}Th/^{238}U and ^{206}Pb/^{238}U ratios after the closure of the U–Pb system. Shading represents the area in which the intersection of the ^{206}Pb/^{238}U and ^{230}Th/^{238}U growth curves falls when $0 < f_{Th/U} < 1$. (b) The growth of (^{230}Th)/(^{238}U) activity slows down over time. Error amplification as the (^{238}U)/(^{230}Th) activities gradually stabilize.

half-lives of ^{230}Th) and the difference between the ^{206}Pb/^{238}U and ^{230}Th/^{238}U ratios continues to increase approaching secular equilibrium. The ^{238}U–^{230}Th system can accumulate more daughter isotopes due to the short half-life when the zircon is younger than *ca.* 150 ka. However, the error multiplication effect on ^{238}U–^{230}Th dating becomes more pronounced as the (^{238}U)/(^{230}Th) activities stabilize gradually after two ^{230}Th half-lives (Fig. 4b). At this point, the radiogenic Pb has increased significantly and the ^{238}U–^{206}Pb system is a better dating

method choice. It is noteworthy that the growth curves of $^{206}Pb/^{238}U$ and $^{230}Th/^{238}U$ ratios in zircon are related to the Th/U fractionation between the zircon and magma ($f_{Th/U}$). The shaded field in Fig. 4a represents the range in which the $^{206}Pb/^{238}U$ and $^{230}Th/^{238}U$ growth curves intersect when $0 < f_{Th/U} < 1$.

There are some differences between ^{238}U–^{206}Pb and ^{238}U–^{230}Th dating during SIMS analysis. The analytical precision is positively correlated with the secondary ion signal intensity during SIMS analysis, which mainly depends on the elemental abundance, ion yield, and primary ion beam current. For a given primary ion beam current, the signal intensity can be improved by increasing the elemental abundance and ion yields. However, there are limited variations in the elemental contents of the sample, so it is important to increase the ion yield. Based on previous studies, the Pb^+ yield of zircon is about 20–30 cps ppm^{-1} nA^{-1},[25] which is much higher than that of Th^+ (4 cps ppm^{-1} nA^{-1}),[26] when oxygen flooding and a primary O_2^- beam are used. In order to improve the precision of Th measurements, Th oxide (ThO^+) is usually analyzed.[27] The yield of ThO^+ is around 50 cps ppm^{-1} nA^{-1},[26] which is significantly higher than that of Th^+ and greatly improves the precision of Th measurements. The accumulation of radiogenic ^{230}Th in zircons younger than *ca.* 150 ka is higher than that of radiogenic ^{206}Pb, which, along with the higher yield of ThO^+ than Pb^+ during SIMS analysis, makes the ^{238}U–^{230}Th system more appropriate for dating zircon in this age range.

Potential interference during SIMS measurements is another important factor that can affect dating results. During zircon ^{238}U–^{206}Pb dating, heavy rare earth elements, Er, Yb, and Lu, and Hf, O, and Si can combine to form polyatomic interferents with mass numbers similar to those of Pb. These interferents can be filtered out when the mass resolution power of the instrument is >5000 (1% peak height). Interferents on ^{204}Pb include $^{186}W^{18}O$ (*e.g.*, cassiterite dating) and $^{232}Th^{144}Nd^{16}O_2^{2+}$ (*e.g.*, high-Th monazite and allanite dating) that cannot be filtered out, but for ^{206}Pb and ^{207}Pb, no interferents have been found at a mass resolution of >5000.[28] The $^{230}ThO^+$ signal is crucial for ion microprobe ^{238}U–^{230}Th dating, and possible interferents include $^{197}AuO_3H^+$ from the gold coating and the polyatomic interferent of $^{232}Th_2{}^{12}C^{16}O^{2+}$ due to the partial overlap of the ion beam on the resin.[7] The former can be filtered out at a mass resolution of >5000, whereas the latter is hard to resolve (*i.e.*, it requires a mass resolution of >40 000). The use of indium metal instead of epoxy resin can partly eliminate the influence of the latter interference, but the possible presence of C-containing inclusions (*e.g.*, graphite and calcite) cannot be excluded.

In summary, the ^{238}U–^{230}Th and ^{238}U–^{206}Pb systems both have advantages and disadvantages when dating zircons in U-series disequilibrium. The largest obstacle to zircon ^{238}U–^{206}Pb dating in U-series disequilibrium is the very low radiogenic Pb content in young zircons. This can be overcome by selecting suitable zircon grains and improving the analytical precision. We suggest that the ^{238}U–^{206}Pb dating method can yield good results for zircon grains with $f_{206} < 0.3$[25] and requires a compromise between common lead and U contents. The use of the multiple-collector mode during SIMS analysis is required to obtain the best precision.[17]

5. Conclusions

We have developed theoretical and analytical methods for zircon U–Pb dating within the age range of U-series disequilibrium, including corrections for initial ^{230}Th disequilibrium related to the $^{206}Pb/^{238}U$ and $^{207}Pb/^{206}Pb$ ratios used for common Pb correction. To verify our method, we dated young zircons from the YTT, which yielded ages similar to those obtained by the ^{238}U–^{230}Th method, but with a significant improvement in precision. From a theoretical and practical perspective, the ^{238}U–^{230}Th method is best suited for zircons younger than 150 ka and requires a high zircon U content and large Th/U fractionation between the magma and zircon. The ^{238}U–^{206}Pb method is advantageous for samples older than 150 ka, but requires a low common Pb content in zircon.

Conflicts of interest

There are no conflicts to declare.

Acknowledgements

We thank H. X. Ma for zircon mounting. We are grateful to Dr Xiaoping Xia and one anonymous reviewer who helped to improve the content and presentation. This research was funded by the National Key R&D Program of China (2018YFA0702600) and National Natural Science Foundation of China (Grants 41773044 and 41773047).

References

1 M. R. Reid, C. D. Coath, T. M. Harrison and K. D. McKeegan, *Earth Planet. Sci. Lett.*, 1997, **150**, 27–39.
2 D. Szymanowski, J.-F. Wotzlaw, B. S. Ellis, O. Bachmann, M. Guillong and A. von Quadt, *Nat. Geosci.*, 2017, **10**, 777–782.
3 M. R. Reid, *Elements*, 2008, **4**, 23–28.
4 M. R. Reid and J. A. Vazquez, *Geochem., Geophys., Geosyst.*, 2017, **18**, 156–177.
5 H. Bateman, *Proc. Cambridge Philos. Soc.*, 1908, **1908**(15), 423–427.
6 J. A. Vazquez and M. R. Reid, *Contrib. Mineral. Petrol.*, 2002, **144**, 274–285.
7 A. K. Schmitt, D. F. Stockli and B. P. Hausback, *J. Volcanol. Geotherm. Res.*, 2006, **158**, 281–295.
8 M. Guillong, A. von Quadt, S. Sakata, I. Peytcheva and O. Bachmann, *J. Anal. At. Spectrom.*, 2014, **29**, 963–970.
9 U. Schärer, *Earth Planet. Sci. Lett.*, 1984, **67**, 191–204.
10 A. K. Schmitt, M. Grove, T. M. Harrison, O. Lovera, J. Hulen and M. Walters, *Geochim. Cosmochim. Acta*, 2003, **67**, 3423–3442.
11 J. t. Stacey and J. Kramers, *Earth Planet. Sci. Lett.*, 1975, **26**, 207–221.

12 S. Nishimura, E. Abe, T. Yokoyama, S. Wirasantosa and A. Dharma, *Paleolimnol. Lake Biwa Jpn. Pleistocene*, 1977, **5**, 313–332.
13 J. Diehl, T. C. Onstott, C. Chesner and M. Knight, *Geophys. Res. Lett.*, 1987, **14**, 753–756.
14 C. A. Chesner, W. I. Rose, A. Deino, R. Drake and J. Westgate, *Geology*, 1991, **19**, 200–203.
15 D. F. Mark, M. Petraglia, V. C. Smith, L. E. Morgan, D. N. Barfod, B. S. Ellis, N. J. Pearce, J. Pal and R. Korisettar, *Quat. Geochronol.*, 2014, **21**, 90–103.
16 C. A. Chesner, *Quat. Int.*, 2012, **258**, 5–18.
17 X.-H. Li, Y. Liu, Q.-L. Li, C.-H. Guo and K. R. Chamberlain, *Geochem., Geophys., Geosyst.*, 2009, **10**, Q04010.
18 M. Whitehouse, S. Claesson, T. Sunde and J. Vestin, *Geochim. Cosmochim. Acta*, 1997, **61**, 4429–4438.
19 Y. Liu, Q.-L. Li, G.-Q. Tang, X.-H. Li and Q.-Z. Yin, *J. Anal. At. Spectrom.*, 2015, **30**, 979–985.
20 J. Hiess, D. J. Condon, N. McLean and S. R. Noble, *Science*, 2012, **335**, 1610–1614.
21 X. Li, G. Tang, B. Gong, Y. Yang, K. Hou, Z. Hu, Q. Li, Y. Liu and W. Li, *Chin. Sci. Bull.*, 2013, **58**, 4647–4654.
22 L. Heaman and A. LeCheminant, *Chem. Geol.*, 2001, **172**, 77–93.
23 J. Blundy and B. Wood, *Earth Planet. Sci. Lett.*, 2003, **210**, 383–397.
24 A. K. Schmitt, *Am. Mineral.*, 2007, **92**, 691–694.
25 Y. Liu, X.-H. Li, Q.-L. Li, G.-Q. Tang and Q.-Z. Yin, *J. Anal. At. Spectrom.*, 2011, **26**, 845–851.
26 Q. Li, Y. Liu, G. Tang, K. Wang, X. Ling and J. Li, *J. Anal. At. Spectrom.*, 2018, **33**, 1536–1544.
27 I. N. Bindeman, A. K. Schmitt and J. W. Valley, *Contrib. Mineral. Petrol.*, 2006, **152**, 649–665.
28 T. Tsunogae and H. Yurimoto, *Geochem. J.*, 1995, **29**, 197–205.